




Editorial

Recent Progress in Quantitative Land Remote Sensing in China

Shunlin Liang ^{1,2,3,*} , Jiancheng Shi ^{1,4}  and Guangjian Yan ^{1,4} 

¹ State Key Laboratory of Remote Sensing Science, Beijing Normal University and Institute of Remote Sensing and Digital Earth, Beijing 100875, China; shijc@radi.ac.cn (J.S.); gjyan@bnu.edu.cn (G.Y.)

² Department of Geographical Sciences, University of Maryland, College Park, MD 20742, USA

³ School of Remote Sensing Information Engineering, Wuhan University, Wuhan 430072, China

⁴ School of Remote Sensing Science and Engineering, Faculty of Geographical Science, Beijing Normal University, Beijing 100875, China

* Correspondence: sliang@umd.edu; Tel.: +1-301-405-4556

Received: 12 September 2018; Accepted: 14 September 2018; Published: 18 September 2018



During the past forty years, since the first book with a title mentioning quantitative and remote sensing was published [1], quantitative land remote sensing has advanced dramatically, and numerous books have been published since then [2–6] although some of them did not use quantitative land remote sensing in their titles. Quantitative land remote sensing has not been explicitly defined in the literature, but we consider it as a sub-discipline of remote sensing including the following components (see Figure 1): radiometric preprocessing, inversion, high-level product generation, and applications. Many inversion algorithms rely on physical models of radiation regimes of landscapes, which link with remotely-sensed data. Generating high-level satellite products of land surface biophysical and biochemical variables create the key bridge between remote sensing science and applications. Conducting in situ measurements for validation of inversion algorithms and satellite products is also a critical component. Application of satellite products to address scientific and societal relevant issues will ultimately decide the future of quantitative land remote sensing.

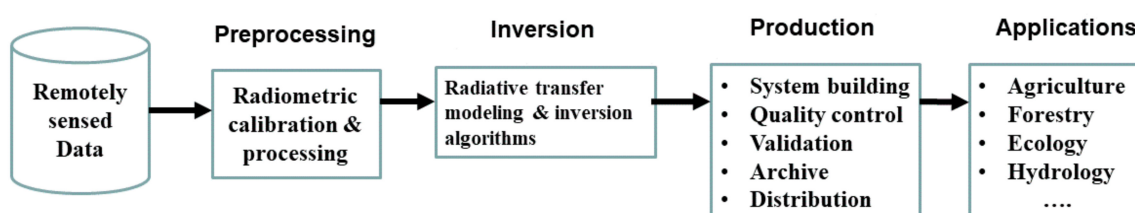


Figure 1. The scope of quantitative land remote sensing.

One of the major drivers of the rapid development of quantitative remote sensing in China is the availability of a huge amount of satellite data not only from the international space agencies but also from Chinese satellite sensors. Figure 2 shows the major Chinese satellite missions for land surface monitoring, such as the China-Brazil Earth resource satellites (CBERS), environment (Huang-Jing, HJ), resources (Zhi-Yuan, ZY), meteorological (Feng-Yun, FY), and high-resolution (Gao-Fen, GF) satellite series. Most of them are polar-orbiting satellites, but GF-5 and FY-4 are geostationary satellites. With the constellation of multiple satellites, both high spatial and temporal resolutions are being achieved.

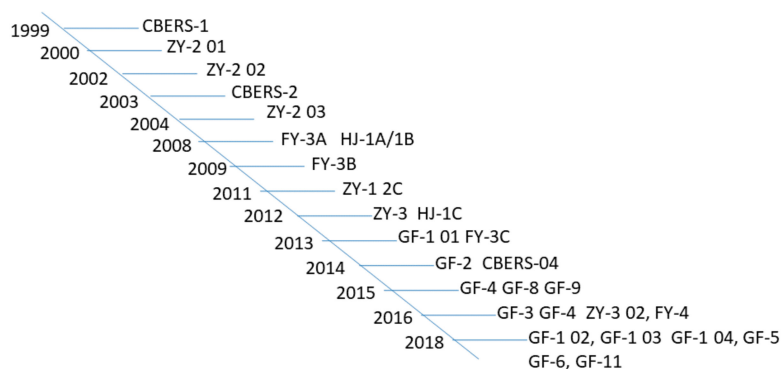


Figure 2. Major Chinese satellites relevant to land remote sensing.

Because of the increased data volume and sophistication of information extraction, one of the trends in quantitative remote sensing is the production of high-level satellite products, mostly by the data centers with centralized facilities and specialized experts. It started from the NASA Earth Observing System (EOS) program in the 1990s. Since then, China has started to produce and distribute satellite products worldwide. One of the major product suites is the Global Land Surface Satellite (GLASS) products [7,8]. It has been expanded from the original 5 products into the present 12 products (see Table 1) that are being distributed free of charge through the China National Data Sharing Infrastructure of Earth System Science (<http://www.geodata.cn/thematicView/GLASS.html>) and the Global Land Cover Facility at the University of Maryland (<http://glcf.umd.edu/data>).

The GLASS products have some unique features, for example, long-time times series (several products span from 1981 to present), high-spatial resolution of the radiation products (5 km instead of the typical resolutions of ~100 km), and high quality and accuracy [9–11]. Efforts are being made in China [12] to develop more Climate Data Records (CDR) that are defined as the time series of measurements of sufficient length, consistency, and continuity to determine climate variability and change by the National Research Council [13].

Table 1. Overview of the Global Land Surface Satellite (GLASS) products and their characteristics.

No.	Product	Spatial Resolution	Temporal Resolution	Temporal Range	References
1	Leaf area index	1–5 km, 0.05°	8 days	1981–2017	[14,15]
2	Albedo	1–5 km, 0.05°	8 days	1981–2017	[16–18]
3	Emissivity	1–5 km, 0.05°	8 days	1981–2017	[19,20]
4	FAPAR	1–5 km, 0.05°	8 days	1981–2017	[21]
5	Downward shortwave radiation	0.05°	1 day	1983, 1993, 2000–2017	[22]
6	PAR	0.05°	1 day	1983, 1993, 2000–2017	[22]
7	Longwave net radiation	0.05°	Instantaneous	1983, 1993, 2003, 2013	[23,24]
8	All-wave net radiation	0.05°	1 day	1983, 1993, 2000–2017	[25]
9	Land Surface Temperature	1–5 km, 0.05°	Instantaneous	1983, 1993, 2003, 2013	[26]
10	Fraction of vegetation cover	500 m, 0.05°	8 days	1981–2017	[27]
11	Latent heat (ET)	1–5 km, 0.05°	8 days	1981–2017	[28]
12	Gross Primary Productivity	1–5 km, 0.05°	8 days	1981–2017	[29]

Many members of our community have made significant contributions to the development of quantitative land remote sensing. Professor Xiaowen Li was one of leading figures. Trained as an electrical engineer, Professor Li started to work on physical modeling of the vegetation radiation

field in the early 1980s under the supervision of Professor Alan Strahler. He developed the well-known Li–Strahler geometric-optical vegetation reflectance model [30,31], and later coupled it with radiative transfer modeling [32,33]. He pioneered the simplified “kernels” to model land surface directional reflectance for developing the MODIS surface albedo products [34]. These “kernels” have been widely used for analyzing various satellite observations. He also explored the angular behavior and scaling of the thermal-infrared remote sensing signatures [35], and proposed to constrain the remote sensing inversion using prior knowledge [36]. In the second half of his career, Professor Li devoted his time and energy to facilitate and promote quantitative land remote sensing research in China by leading several extensive research projects, directing the Research Institute on Remote Sensing under the Chinese Academy of Sciences, and helping establish the State Key Laboratory of Remote Sensing Science under the Chinese Ministry of Science and Technology. Those are just few examples of areas where Professor Li has made outstanding contributions. A comprehensive summary of his achievements has been provided by Liu et al. [37].

In memory of Professor Li, we organized the Third National Forum on Quantitative Remote Sensing at Beijing Normal University during 14–15 July 2017. There were 296 meeting participants from 65 research institutes and universities in China, and almost all aspects of quantitative land remote sensing were discussed.

The papers of this Special Issue are mainly from this forum. Although 40 articles cannot comprehensively characterize different aspects of quantitative land remote sensing in China, they clearly represent the current level of research in this area by Chinese scientists. These papers are related to various satellite data products, such as incident solar radiation [38–40], chlorophyll fluorescence [41], surface directional reflectance [42–44], aerosol optical depth [45], albedo [46,47], land surface temperature [48–50], upward longwave radiation [51], leaf area index [52–55], fractional vegetation cover [56], forest biomass [57], precipitation [58], evapotranspiration [59–61], freeze/thaw [62], snow cover [63], vegetation productivity [64–68], phenology [69,70], biodiversity indicators [71], drought monitoring [72], forest disturbance [55], air-quality monitoring [73], sensor design [74], and sampling strategy [75] for validation with in situ measurements. Most of these papers are based on optical-thermal remotely-sensed observations, but a few papers are also based on microwave [62,63] and Lidar [54,76] data.

Although these 40 papers do not represent a large sample, they demonstrate that few studies have been undertaken on physical modeling for understanding remotely-sensed signals and use of Chinese satellite data in their analysis. This latter shortcoming calls for the further improvement of Chinese satellite data quality.

Acknowledgments: This work was supported in part by the National Key Research and Development Program of China (No. 2016YFA0600101) and the National Natural Science Foundation of China (No. 41331173). We would like to thank the members of the Scientific Steering Committee and the Organizing Committee of the Third National Forum on Quantitative Remote Sensing at Beijing Normal University for their great contributions.

Conflicts of Interest: The authors declare no conflicts of interest

References

1. Swain, P.H.; Shirley, M.D. *Remote Sensing: The Quantitative Approach*; McGraw Hill: New York, NY, USA, 1978.
2. Liang, S. *Quantitative Remote Sensing of Land Surfaces*; John Wiley & Sons, Inc.: New York, NY, USA, 2004.
3. Liang, S. *Advances in Land Remote Sensing: System, Modeling, Inversion and Application*; Springer: New York, NY, USA, 2008.
4. Liang, S.; Li, X.; Wang, J. *Advanced Remote Sensing: Terrestrial Information Extraction and Applications*; Elsevier Science Bv: Amsterdam, The Netherlands, 2012.
5. Myneni, R.; Ross, J. *Photon-Vegetation Interactions: Applications in Optical Remote Sensing and Plant Ecology*; Springer: Berlin/Heidelberg, Germany, 1991.
6. Tang, H.; Li, Z.L. *Quantitative Remote Sensing in Thermal Infrared: Theory and Applications*; Springer: Berlin, Germany, 2014.

7. Liang, S.; Zhang, X.; Xiao, Z.; Cheng, J.; Liu, Q.; Zhao, X. *Global LAnd Surface Satellite (GLASS) Products: Algorithms, Validation and Analysis*; Springer: Berlin, Germany, 2013.
8. Liang, S.; Zhao, X.; Yuan, W.; Liu, S.; Cheng, X.; Xiao, Z.; Zhang, X.; Liu, Q.; Cheng, J.; Tang, H.; et al. A long-term global land surface satellite (GLASS) dataset for environmental studies. *Int. J. Digit. Earth* **2013**, *6*, 5–33. [[CrossRef](#)]
9. Xiao, Z.; Liang, S.; Jiang, B. Evaluation of four long time-series global leaf area index products. *Agric. For. Meteorol.* **2017**, *246*, 218–230. [[CrossRef](#)]
10. Xiao, Z.; Liang, S.; Sun, R. Evaluation of three long time series for global fraction of absorbed photosynthetically active radiation (fapar) products. *IEEE Trans. Geosci. Remote Sens.* **2018**, *56*, 5509–5524. [[CrossRef](#)]
11. Xu, B.; Li, J.; Park, T.; Liu, Q.; Zeng, Y.; Yin, G.; Zhao, J.; Fan, W.; Yang, L.; Knyazikhin, Y.; et al. An integrated method for validating long-term leaf area index products using global networks of site-based measurements. *Remote Sens. Environ.* **2018**, *209*, 134–151. [[CrossRef](#)]
12. Liang, S.; Tang, S.; Zhang, J.; Xu, B.; Cheng, J.; Cheng, X. Production of the global climate data records and applications to climate change studies. *J. Remote Sens.* **2016**, *20*, 1401–1499.
13. NRC. *Climate Data Records from Environmental Satellites: Interim Report*; The National Academies Press: Washington, DC, USA, 2004.
14. Xiao, Z.; Liang, S.; Wang, J.; Xiang, Y.; Zhao, X.; Song, J. Long-time-series global land surface satellite leaf area index product derived from MODIS and AVHRR surface reflectance. *IEEE Trans. Geosci. Remote Sens.* **2016**, *54*, 5301–5318. [[CrossRef](#)]
15. Xiao, Z.Q.; Liang, S.; Wang, J.D.; Chen, P.; Yin, X.J.; Zhang, L.Q.; Song, J.L. Use of general regression neural networks for generating the GLASS leaf area index product from time-series MODIS surface reflectance. *IEEE Trans. Geosci. Remote Sens.* **2014**, *52*, 209–223. [[CrossRef](#)]
16. Qu, Y.; Liu, Q.; Liang, S.; Wang, L.; Liu, N.; Liu, S. Improved direct-estimation algorithm for mapping daily land-surface broadband albedo from MODIS data. *IEEE Trans. Geosci. Remote Sens.* **2014**, *52*, 907–919. [[CrossRef](#)]
17. Liu, N.; Liu, Q.; Wang, L.; Liang, S.; Wen, J.; Qu, Y.; Liu, S.H. A statistics-based temporal filter algorithm to map spatiotemporally continuous shortwave albedo from MODIS data. *Hydrol. Earth Syst. Sci.* **2013**, *17*, 2121–2129. [[CrossRef](#)]
18. Liu, Q.; Wang, L.; Qu, Y.; Liu, N.; Liu, S.; Tang, H.; Liang, S. Primary evaluation of the long-term GLASS albedo product. *Int. J. Digit. Earth* **2013**, *6*, 69–95. [[CrossRef](#)]
19. Cheng, J.; Liang, S. A novel algorithm for estimating broadband emissivity of global bare soil using MODIS albedo product. *IEEE Trans. Geosci. Remote Sens.* **2013**, *51*, 2619–2631.
20. Cheng, J.; Liang, S.; Verhoef, W.; Shi, L.; Liu, Q. Estimating the hemispherical broadband longwave emissivity of global vegetated surfaces using a radiative transfer model. *IEEE Trans. Geosci. Remote Sens.* **2016**, *54*, 905–917. [[CrossRef](#)]
21. Xiao, Z.; Liang, S.; Sun, R.; Wang, J.; Jiang, B. Estimating the fraction of absorbed photosynthetically active radiation from the MODIS data based GLASS leaf area index product. *Remote Sens. Environ.* **2015**, *171*, 105–117. [[CrossRef](#)]
22. Zhang, X.; Liang, S.; Zhou, G.; Wu, H.; Zhao, X. Generating global land surface satellite incident shortwave radiation and photosynthetically active radiation products from multiple satellite data. *Remote Sens. Environ.* **2014**, *152*, 318–332. [[CrossRef](#)]
23. Cheng, J.; Liang, S. Global estimates for high-spatial-resolution clear-sky land surface upwelling longwave radiation from MODIS data. *IEEE Trans. Geosci. Remote Sens.* **2016**, *54*, 4115–4129. [[CrossRef](#)]
24. Cheng, J.; Liang, S.; Wang, W.; Guo, Y. An efficient hybrid method for estimating clear-sky surface downward longwave radiation from MODIS data. *J. Geophys. Res. Atmos.* **2017**, *122*, 2616–2630. [[CrossRef](#)]
25. Jiang, B.; Liang, S.; Ma, H.; Zhang, X.; Xiao, Z.; Zhao, X.; Jia, K.; Yao, Y.; Jia, A. GLASS daytime all-wave net radiation product: Algorithm development and preliminary validation. *Remote Sens.* **2016**, *8*, 222. [[CrossRef](#)]
26. Zhou, J.; Zhang, X.; Zhan, W.; Zhang, H. Land surface temperature retrieval from MODIS data by integrating regression models and the genetic algorithm in an arid region. *Remote Sens.* **2014**, *6*, 5344–5367. [[CrossRef](#)]
27. Jia, K.; Liang, S.; Liu, S.H.; Li, Y.W.; Xiao, Z.Q.; Yao, Y.J.; Jiang, B.; Zhao, X.; Wang, X.; Xu, S.; et al. Global land surface fractional vegetation cover estimation using general regression neural networks from MODIS surface reflectance. *IEEE Trans. Geosci. Remote Sens.* **2015**, *53*, 4787–4796. [[CrossRef](#)]

28. Yao, Y.; Liang, S.; Li, X.; Hong, Y.; Fisher, J.B.; Zhang, N.; Chen, J.; Cheng, J.; Zhao, S.; Zhang, X.; et al. Bayesian multimodel estimation of global terrestrial latent heat flux from eddy covariance, meteorological, and satellite observations. *J. Geophys. Res. Atmos.* **2014**, *119*, 4521–4545. [[CrossRef](#)]
29. Yuan, W.P.; Liu, S.; Zhou, G.S.; Zhou, G.Y.; Tieszen, L.L.; Baldocchi, D.; Bernhofer, C.; Gholz, H.; Goulden, M.L.; Hollinger, D.Y.; et al. Deriving a light use efficiency model from eddy covariance flux data for predicting daily gross primary production across biomes. *Agric. For. Meteorol.* **2007**, *143*, 189–207. [[CrossRef](#)]
30. Li, X.; Strahler, A. Geometric-optical modeling of a coniferous forest canopy. *IEEE Trans. Geosci. Remote Sens.* **1985**, *23*, 705–721. [[CrossRef](#)]
31. Li, X.; Strahler, A. Geometric-optical bi-directional reflectance modeling of a coniferous forest canopy. *IEEE Trans. Geosci. Remote Sens.* **1986**, *24*, 906–919. [[CrossRef](#)]
32. Li, X.; Strahler, A.H. Geometric-optical bidirectional reflectance modeling of the discrete crown vegetation canopy: Effect of crown shape and mutual shadowing. *IEEE Trans. Geosci. Remote Sens.* **1992**, *30*, 276–292. [[CrossRef](#)]
33. Li, X.; Strahler, A.H.; Woodcock, C.E. A hybrid geometric optical-radiative transfer approach for modeling albedo and directional reflectance of discontinuous canopies. *IEEE Trans. Geosci. Remote Sens.* **1995**, *33*, 466–480.
34. Wanner, W.; Li, X.; Strahler, A. On the derivation of kernels for kernel-driven models of bidirectional reflectance. *J. Geophys. Res. Atmos.* **1995**, *100*, 21077–21089. [[CrossRef](#)]
35. Li, X.; Strahler, A.H.; Friedl, M.A. A conceptual model for effective directional emissivity from nonisothermal surfaces. *IEEE Trans. Geosci. Remote Sens.* **1999**, *37*, 2508–2517.
36. Li, X.; Gao, F.; Wang, J.; Strahler, A. A priori knowledge accumulation and its application to linear BRDF model inversion. *J. Geophys. Res. Atmos.* **2001**, *106*, 11925–11935. [[CrossRef](#)]
37. Liu, Q.; Yan, G.; Jiao, Z.; Wen, J.; Liang, S.; Wang, J. From geometric-optical optical remote sensing modeling to quantitative remote sensing science—In memory of Academician Xiaowen Li. *Remote Sens.* **2018**. new submit.
38. Yang, L.; Zhang, X.; Liang, S.; Yao, Y.; Jia, K.; Jia, A. Estimating surface downward shortwave radiation over china based on the gradient boosting decision tree method. *Remote Sens.* **2018**, *10*, 185. [[CrossRef](#)]
39. Zhang, H.; Huang, C.; Yu, S.; Li, L.; Xin, X.; Liu, Q. A lookup-table-based approach to estimating surface solar irradiance from geostationary and polar-orbiting satellite data. *Remote Sens.* **2018**, *10*, 411. [[CrossRef](#)]
40. Zhou, Y.; Yan, G.; Zhao, J.; Chu, Q.; Liu, Y.; Yan, K.; Tong, Y.; Mu, X.; Xie, D.; Zhang, W. Estimation of daily average downward shortwave radiation over antarctica. *Remote Sens.* **2018**, *10*, 422. [[CrossRef](#)]
41. Hu, J.; Liu, X.; Liu, L.; Guan, L. Evaluating the performance of the SCOPE model in simulating canopy solar-induced chlorophyll fluorescence. *Remote Sens.* **2018**, *10*, 250. [[CrossRef](#)]
42. Wu, Q.; Song, C.; Song, J.; Wang, J.; Chen, S.; Yu, B. Impacts of leaf age on canopy spectral signature variation in evergreen Chinese fir forests. *Remote Sens.* **2018**, *10*, 262. [[CrossRef](#)]
43. Wen, J.; Liu, Q.; Xiao, Q.; Liu, Q.; You, D.; Hao, D.; Wu, S.; Lin, X. Characterizing land surface anisotropic reflectance over rugged terrain: A review of concepts and recent developments. *Remote Sens.* **2018**, *10*, 370. [[CrossRef](#)]
44. Zhang, C.; Ren, H.; Liang, Y.; Liu, S.; Qin, Q.; Ersoy, O. Advancing the prospect-5 model to simulate the spectral reflectance of copper-stressed leaves. *Remote Sens.* **2017**, *9*, 1191. [[CrossRef](#)]
45. Tian, X.; Liu, S.; Sun, L.; Liu, Q. Retrieval of aerosol optical depth in the arid or semiarid region of Northern Xinjiang, China. *Remote Sens.* **2018**, *10*, 197. [[CrossRef](#)]
46. Lin, X.; Wen, J.; Liu, Q.; Xiao, Q.; You, D.; Wu, S.; Hao, D.; Wu, X. A multi-scale validation strategy for albedo products over rugged terrain and preliminary application in Heihe River Basin, China. *Remote Sens.* **2018**, *10*, 156. [[CrossRef](#)]
47. Hao, D.; Wen, J.; Xiao, Q.; Wu, S.; Lin, X.; Dou, B.; You, D.; Tang, Y. Simulation and analysis of the topographic effects on snow-free albedo over rugged terrain. *Remote Sens.* **2018**, *10*, 278. [[CrossRef](#)]
48. Tang, B.; Zhao, X.; Zhao, W. Local effects of forests on temperatures across Europe. *Remote Sens.* **2018**, *10*, 529. [[CrossRef](#)]
49. Yu, W.; Ma, M.; Li, Z.; Tan, J.; Wu, A. New scheme for validating remote-sensing land surface temperature products with station observations. *Remote Sens.* **2017**, *9*, 1210. [[CrossRef](#)]
50. Meng, X.; Cheng, J.; Liang, S. Estimating land surface temperature from feng yun-3C/MERSI data using a new land surface emissivity scheme. *Remote Sens.* **2017**, *9*, 1247. [[CrossRef](#)]

51. Zhou, S.; Cheng, J. Estimation of high spatial-resolution clear-sky land surface-upwelling longwave radiation from VIIRS/S-NPP data. *Remote Sens.* **2018**, *10*, 253. [[CrossRef](#)]
52. Zhao, J.; Li, J.; Liu, Q.; Wang, H.; Chen, C.; Xu, B.; Wu, S. Comparative analysis of Chinese HJ-1 CCD, GF-1 WFV and ZY-3 MUX sensor data for leaf area index estimations for maize. *Remote Sens.* **2018**, *10*, 68. [[CrossRef](#)]
53. Zhou, J.; Zhang, S.; Yang, H.; Xiao, Z.; Gao, F. The retrieval of 30-m resolution LAI from landsat data by combining MODIS products. *Remote Sens.* **2018**, *10*, 1187. [[CrossRef](#)]
54. Li, S.; Dai, L.; Wang, H.; Wang, Y.; He, Z.; Lin, S. Estimating leaf area density of individual trees using the point cloud segmentation of terrestrial LiDAR data and a voxel-based model. *Remote Sens.* **2017**, *9*, 1202. [[CrossRef](#)]
55. Wang, J.; Wang, J.; Zhou, H.; Xiao, Z. Detecting forest disturbance in northeast China from GLASS LAI time series data using a dynamic model. *Remote Sens.* **2017**, *9*, 1293. [[CrossRef](#)]
56. Yang, L.; Jia, K.; Liang, S.; Liu, M.; Wei, X.; Yao, Y.; Zhang, X.; Liu, D. Spatio-temporal analysis and uncertainty of fractional vegetation cover change over northern China during 2001–2012 based on multiple vegetation data sets. *Remote Sens.* **2018**, *10*, 549. [[CrossRef](#)]
57. Wang, M.; Sun, R.; Xiao, Z. Estimation of forest canopy height and aboveground biomass from spaceborne LiDAR and landsat imageries in Maryland. *Remote Sens.* **2018**, *10*, 344. [[CrossRef](#)]
58. Zeng, Q.; Wang, Y.; Chen, L.; Wang, Z.; Zhu, H.; Li, B. Inter-comparison and evaluation of remote sensing precipitation products over China from 2005 to 2013. *Remote Sens.* **2018**, *10*, 168. [[CrossRef](#)]
59. Li, X.; Xin, X.; Peng, Z.; Zhang, H.; Yi, C.; Li, B. Analysis of the spatial variability of land surface variables for ET estimation: Case study in HiWATER Campaign. *Remote Sens.* **2018**, *10*, 91. [[CrossRef](#)]
60. Zhang, L.; Yao, Y.; Wang, Z.; Jia, K.; Zhang, X.; Zhang, Y.; Wang, X.; Xu, J.; Chen, X. Satellite-derived spatiotemporal variations in evapotranspiration over northeast China during 1982–2010. *Remote Sens.* **2017**, *9*, 1140. [[CrossRef](#)]
61. Wang, X.; Yao, Y.; Zhao, S.; Jia, K.; Zhang, X.; Zhang, Y.; Zhang, L.; Xu, J.; Chen, X. MODIS-based estimation of terrestrial latent heat flux over north america using three machine learning algorithms. *Remote Sens.* **2017**, *9*, 1326. [[CrossRef](#)]
62. Hu, T.; Zhao, T.; Shi, J.; Wu, S.; Liu, D.; Qin, H.; Zhao, K. High-resolution mapping of freeze/thaw status in china via fusion of MODIS and AMSR2 data. *Remote Sens.* **2017**, *9*, 1339. [[CrossRef](#)]
63. Liu, X.; Jiang, L.; Wu, S.; Hao, S.; Wang, G.; Yang, J. Assessment of methods for passive microwave snow cover mapping using FY-3C/MWRI data in China. *Remote Sens.* **2018**, *10*, 524. [[CrossRef](#)]
64. Yu, T.; Sun, R.; Xiao, Z.; Zhang, Q.; Liu, G.; Cui, T.; Wang, J. Estimation of global vegetation productivity from global land surface satellite data. *Remote Sens.* **2018**, *10*, 327. [[CrossRef](#)]
65. Hu, L.; Fan, W.; Ren, H.; Liu, S.; Cui, Y.; Zhao, P. Spatiotemporal dynamics in vegetation GPP over the great khingan mountains using GLASS products from 1982 to 2015. *Remote Sens.* **2018**, *10*, 488. [[CrossRef](#)]
66. Xie, X.; Li, A.; Jin, H.; Yin, G.; Bian, J. Spatial downscaling of gross primary productivity using topographic and vegetation heterogeneity information: A case study in the Gongga Mountain Region of China. *Remote Sens.* **2018**, *10*, 647. [[CrossRef](#)]
67. Lin, S.; Li, J.; Liu, Q.; Huete, A.; Li, L. Effects of forest canopy vertical stratification on the estimation of gross primary production by remote sensing. *Remote Sens.* **2018**, *10*, 1329. [[CrossRef](#)]
68. Cui, T.; Sun, R.; Qiao, C.; Zhang, Q.; Yu, T.; Liu, G.; Liu, Z. Estimating diurnal courses of gross primary production for maize: A comparison of sun-induced chlorophyll fluorescence, light-use efficiency and process-based models. *Remote Sens.* **2017**, *9*, 1267. [[CrossRef](#)]
69. He, Z.; Li, S.; Wang, Y.; Dai, L.; Lin, S. Monitoring rice phenology based on backscattering characteristics of multi-temporal RADARSAT-2 datasets. *Remote Sens.* **2018**, *10*, 340. [[CrossRef](#)]
70. Zheng, Z.; Zhu, W. Uncertainty of remote sensing data in monitoring vegetation phenology: A comparison of MODIS C5 and C6 vegetation index products on the Tibetan Plateau. *Remote Sens.* **2017**, *9*, 1288. [[CrossRef](#)]
71. Wu, J.; Liang, S. Developing an integrated remote sensing based biodiversity index for predicting animal species richness. *Remote Sens.* **2018**, *10*, 739. [[CrossRef](#)]
72. Xia, L.; Zhao, F.; Mao, K.; Yuan, Z.; Zuo, Z.; Xu, T. SPI-based analyses of drought changes over the past 60 years in China's major crop-growing areas. *Remote Sens.* **2018**, *10*, 171. [[CrossRef](#)]

73. Yun, G.; Zuo, S.; Dai, S.; Song, X.; Xu, C.; Liao, Y.; Zhao, P.; Chang, W.; Chen, Q.; Li, Y.; et al. Individual and interactive influences of anthropogenic and ecological factors on forest PM2.5 concentrations at an urban scale. *Remote Sens.* **2018**, *10*, 521. [[CrossRef](#)]
74. Zhou, H.; Wang, J.; Liang, S. Design of a novel spectral albedometer for validating the MODerate resolution imaging spectroradiometer spectral albedo product. *Remote Sens.* **2018**, *10*, 101. [[CrossRef](#)]
75. Yin, G.; Li, A.; Verger, A. Spatiotemporally representative and cost-efficient sampling design for validation activities in wanglang experimental site. *Remote Sens.* **2017**, *9*, 1217. [[CrossRef](#)]
76. Xie, D.; Wang, X.; Qi, J.; Chen, Y.; Mu, X.; Zhang, W.; Yan, G. Reconstruction of Single Tree with Leaves Based on Terrestrial LiDAR Point Cloud Data. *Remote Sens.* **2018**, *10*, 686. [[CrossRef](#)]



© 2018 by the authors. Licensee MDPI, Basel, Switzerland. This article is an open access article distributed under the terms and conditions of the Creative Commons Attribution (CC BY) license (<http://creativecommons.org/licenses/by/4.0/>).